Pharmacokinetics, Tissue Localization, Toxicity, and Treatment Efficacy in the First Small Animal (Rabbit) Model of Intra-Arterial Chemotherapy for Retinoblastoma

Anthony B. Daniels,[1–4] Michael T. Froehler,[5] Janene M. Pierce,[1] Amy H. Nunnally,[1,6] M. Wade Calcutt,[7] Thomas M. Bridges,[8] David C. LaNeve,[6] Phillip E. Williams,[6] Kelli L. Boyd,[4,9] Michelle L. Reyzer,[7] Craig W. Lindsley,[4,8,10] Debra L. Friedman,[4,11] and Ann Richmond[2,4,12]

[1]Department of Ophthalmology and Visual Sciences, Vanderbilt University Medical Center, Nashville, Tennessee, United States
[2]Department of Cancer Biology, Vanderbilt University, Nashville, Tennessee, United States
[3]Department of Radiation Oncology, Vanderbilt University Medical Center, Nashville, Tennessee, United States
[4]Vanderbilt-Ingram Cancer Center, Vanderbilt University Medical Center, Nashville, Tennessee, United States
[5]Cerebrovascular Program, Vanderbilt University Medical Center, Nashville, Tennessee, United States
[6]Surgical Research, Vanderbilt University Medical Center, Nashville, Tennessee, United States
[7]Department of Biochemistry, Vanderbilt University, Nashville, Tennessee, United States
[8]Vanderbilt Center for Neuroscience Drug Discovery, Department of Pharmacology, Vanderbilt University, Nashville, Tennessee, United States
[9]Department of Pathology, Microbiology and Immunology, Vanderbilt University Medical Center, Nashville, Tennessee, United States
[10]Department of Chemistry, Vanderbilt University, Nashville, Tennessee, United States
[11]Department of Pediatrics, Vanderbilt University Medical Center, Nashville, Tennessee, United States
[12]Tennessee Valley Healthcare System, Department of Veterans Affairs, Nashville, Tennessee, United States

Correspondence: Anthony B. Daniels, Vanderbilt Eye Institute, Vanderbilt University Medical Center, 2311 Pierce Avenue, Nashville, TN 37232, USA; anthony.b.daniels@vanderbilt.edu.

Submitted: May 30, 2017
Accepted: December 5, 2017

Citation: Daniels AB, Froehler MT, Pierce JM, et al. Pharmacokinetics, tissue localization, toxicity, and treatment efficacy in the first small animal (rabbit) model of intra-arterial chemotherapy for retinoblastoma. *Invest Ophthalmol Vis Sci*. 2018;59:446–454. https://doi.org/10.1167/iovs.17-22302

Purpose. Current intra-arterial chemotherapy (IAC) drug regimens for retinoblastoma have ocular and vascular toxicities. No small-animal model of IAC exists to test drug efficacy and toxicity in vivo for IAC drug discovery. The purpose of this study was to develop a small-animal model of IAC and to analyze the ocular tissue penetration, distribution, pharmacokinetics, and treatment efficacy.

Methods. Following selective ophthalmic artery (OA) catheterization, melphalan (0.4 to 1.2 mg/kg) was injected. For pharmacokinetic studies, rabbits were euthanized at 0.5, 1, 2, 4, or 6 hours following intra-OA infusion. Drug levels were determined in vitreous, retina, and blood by liquid chromatography tandem mass spectrometry. To assess toxicity, angiograms, photography, fluorescein angiography, and histopathology were performed. For in situ tissue drug distribution, matrix-assisted laser desorption/ionization imaging mass spectrometry (MALDI-IMS) was performed. The tumor model was created by combined subretinal/intravitreal injection of human WERI-Rb1 retinoblastoma cells; the tumor was treated in vivo with intra-arterial melphalan or saline; and induction of tumor death was measured by cleaved caspase-3 activity.

Results. OA was selectively catheterized for 79 of 79 (100%) eyes in 47 of 47 (100%) rabbits, and melphalan was delivered successfully in 31 of 31 (100%) eyes, without evidence of vascular occlusion or retinal damage. For treated eyes, maximum concentration (C_{max}) in the retina was 4.95 μM and area under the curve ($AUC_{0\rightarrow\infty}$) was 5.26 μM·h. Treated eye vitreous C_{max} was 2.24 μM and $AUC_{0\rightarrow\infty}$ was 4.19 μM·h. Vitreous C_{max} for the treated eye was >100-fold higher than for the untreated eye ($P = 0.01$), and $AUC_{0\rightarrow\infty}$ was ~50-fold higher ($P = 0.01$). Histology-directed MALDI-IMS revealed highest drug localization within the retina. Peripheral blood C_{max} was 1.04 μM and $AUC_{0\rightarrow\infty}$ was 2.07 μM·h. Combined subretinal/intravitreal injection of human retinoblastoma cells led to intra-retinal tumors and subretinal/vitreous seeds, which could be effectively killed in vivo with intra-arterial melphalan.

Conclusions. This first small-animal model of IAC has excellent vitreous and retinal tissue drug penetration, achieving levels sufficient to kill human retinoblastoma cells, facilitating future IAC drug discovery.

Keywords: retinoblastoma, pharmacokinetics, animal models, chemotherapy, intra-arterial chemotherapy

Retinoblastoma (RB) is the most common primary intraocular malignancy in children. The mainstay of globe-conserving therapy has been intravenous (IV) chemotherapy.[1,2] In high-income countries, this has allowed patient survival rates near 99%.[3] However, systemic chemotherapy is associated with acute toxicities such as cytopenias, infection, gastrointestinal toxicity, and the need for hospitalization.[1,4–8] In addition, there is long-term potential for organ dysfunction[9–11] and a very small, but yet present, increased risk for subsequent leukemia.[4–6,12–15] It has been shown that eyes with advanced tumors (Reese-Ellsworth [RE] group V and International Classification of Retinoblastoma [ICRB] group D and E) are rarely saved by intravenous chemotherapy and often require enucleation.[16,17] Systemic chemotherapy has particularly poor success against the subretinal and vitreous seeds seen with more advanced tumors.[18] Recently, alternative local approaches for delivering chemotherapy to the eye have been developed,[19,20] which not only minimize systemic concentrations of drug and systemic toxicity,[21,22] but also allow much higher intraocular drug concentrations to be achieved.[23] Intra-arterial chemotherapy (IAC, also known as ophthalmic artery chemosurgery, via a microcatheter advanced endovascularly to the ophthalmic artery),[19] using various melphalan-based regimens,[24] has led to dramatic improvements in globe salvage rates for these advanced eyes, compared to traditional intravenous chemoreduction.[15,25]

Over the last decade, many authors have published their clinical experience with the microcatheter-based IAC technique for the treatment of children with RB, yet animal models of IAC were not described until recently. IAC has recently been performed in pigs[21] and in nonhuman primates,[26] demonstrating its technical feasibility in large animals. However, there are no RB models in these large animals, and thus they do not provide a platform in which the efficacy of intra-arterial chemotherapeutic agents can be assessed. In contrast, models of RB do exist in small animals, including in rabbits.[27] Therefore, a rabbit model of IAC would allow for drug discovery and assessment of efficacy, in a way not possible with current large animal models of IAC.

We describe here our technique for IAC drug delivery in a small animal (rabbit) model, and determine the vitreous and intraretinal tissue pharmacokinetics of melphalan in this model. We demonstrate that high concentrations of melphalan in both the retina and vitreous are achieved for an adequate length of time to be lethal to human RB cells and that melphalan concentrates at higher levels in the retina than in the vitreous following IAC. We also demonstrate the lack of acute and subacute retinal and retinal vascular complications in this model. Last, we describe a rabbit model of retinoblastoma with both intraretinal tumors and subretinal and vitreous seeds, based on the previous RB model of Kang and Grossniklaus, and demonstrate that intra-arterial melphalan can effectively kill human retinoblastoma xenografts.[27]

Methods

Rabbit IAC Technique

All procedures were performed under the auspices of the Vanderbilt Institutional Animal Care and Use Committee (protocol M/15/072) and adhered to the ARVO Statement for the Use of Animals in Ophthalmic and Vision Research. New Zealand white rabbits (3.0 to 3.2 kg) were used for all studies. Anesthesia was induced with intramuscular ketaset/xylazine and maintained with isoflurane via intubation. Femoral arterial access was obtained by cut-down, and the femoral artery was bathed in verapamil. Endovascular access was obtained using a 4-F micropuncture system. The 4-F sheath was sutured in place and connected to a heparinized saline flush. A 1.5-F Marathon microcatheter was advanced over a Mirage microwire (Medtronic Neurovascular, Minneapolis, MN, USA). Under fluoroscopic guidance, the catheter was advanced into the common carotid artery, and an antero-posterior subtraction angiogram was performed. The dominant arterial blood supply to the eye was then assessed, whether from the internal ophthalmic artery (IOA) via the internal carotid artery (ICA) or from the external ophthalmic artery (EOA) via the external carotid artery (ECA). The microcatheter was then navigated to whichever ophthalmic artery (OA) supplied the retinal vasculature in that particular rabbit, and angiography once again confirmed selection of the OA. Vasospasm was treated with intra-arterial nitroglycerin (50 to 100 μg), if needed. Fluorescein angiography could be performed following selective injection of 10% fluorescein sodium (1:100,000) into the OA to demonstrate ophthalmic supply of the selected vessel (PictorPlusFA, Volk Optical Inc., Mentor, OH, USA). Once OA selection was completed, melphalan was prepared according to the manufacturer's specifications and filtered through a 0.22-μm filter prior to use. Melphalan (0.4 mg/kg) was infused in a pulsatile fashion over 5 minute, followed by a saline flush. All melphalan infusions were performed within 1 hour following reconstitution of the melphalan. Angiography was then performed after the IAC infusion to assess for vascular occlusion or embolus. For survival procedures, the sheath was removed from the femoral artery at the end of the procedure, and the artery was then ligated above and below the arteriotomy site to ensure hemostasis. The fascia was sutured closed, followed by subcuticular skin suture closure. For assessment of acute/subacute vascular toxicity, the rabbit was euthanized at 48 hours or 7 days after the procedure, and both eyes were harvested, fixed in Davidson's solution, and submitted for histopathology.

Tissue Acquisition to Determine Retinal Pharmacokinetics

Following intra-OA melphalan infusion, rabbits were euthanized via barbiturate overdose at the 30-minute, 1-hour, 2-hour, 4-hour, and 6-hour time points (three to four rabbits per time point). Immediately prior to euthanasia, peripheral blood was obtained in EDTA tubes, spun down, and plasma was snap-frozen. Vitreous was likewise obtained via 21-gauge needle tap of both the treated and untreated eyes and snap-frozen. The treated eye was removed immediately after euthanasia, and the retina was dissected and snap-frozen.

Determination of Vitreous and Retinal Melphalan Concentrations by Liquid Chromatography Tandem Mass Spectrometry

Vitreous samples were thawed and spiked with an internal carbamazepine standard, diluted with blank plasma, and deproteinized with acetonitrile. For retinal tissue drug levels, the snap-frozen retinal tissue (see above) was weighed, homogenized, and then thawed and spiked with an internal carbamazepine standard, prior to being diluted with blank plasma and deproteinized with acetonitrile. Calibration samples were prepared in parallel by spiking blank plasma with internal standard and known concentrations of melphalan (for melphalan PK experiments) or cyclosporine (to determine the vitreous concentration of cyclosporine in the RB model). Samples were analyzed on a Thermo Scientific TSQ Quantum Ultra mass spectrometer (Waltham, MA, USA) interfaced to a Waters Acquity UPLC system (Milford, MA, USA).

Pharmacokinetic Analysis and Statistical Analysis

Melphalan concentrations from each source (i.e., plasma, treated eye vitreous, untreated eye vitreous, and treated eye retina) were averaged at each time point (three to four rabbits per time point), and the resulting mean time-concentration data from each matrix were analyzed via noncompartmental analysis (Phoenix WinNonlin v6.4; Pharsight/Certara USA Inc., Princeton, NJ, USA) to determine pharmacokinetic (PK) parameters. For comparisons between treated and untreated eyes, a two-sided *t*-test was used for the comparisons of maximum concentration (C_{max}) values. Comparisons of areas under the curve from $0 \rightarrow \infty$ ($AUC_{0 \rightarrow \infty}$) were based on the *t*-distribution with the Satterthwaite degrees of freedom.

Imaging Mass Spectrometry

Thirty minutes following intra-OA infusion of 1.2 mg/kg melphalan, the treated eye was harvested and snap-frozen. The eye was cut on a cryostat into 12-μm-thick sections, which were thaw-mounted on gold-coated stainless steel matrix-assisted laser desorption/ionization (MALDI) target plates. MALDI matrix [α-cyano-4-hydroxycinnamic acid (CHCA); 5 mg/mL in 90% acetonitrile] was homogeneously applied to the sections using an HTX Technologies TM Sprayer (Chapel Hill, NC, USA). Spectra were acquired in an ordered array over the tissue sections at 150-μm resolution using a linear ion trap equipped with a MALDI-source (Thermo LTQ XL; Thermo Fisher Scientific, Waltham, MA, USA). Spectra were acquired in positive ion mode by isolating and fragmenting the precursor melphalan ion at m/z 305 and detecting the main fragment ion at m/z 168. The intensity of the drug could be plotted as a two-dimensional ion image, showing the localization and relative intensity of the drug in the eye tissue. A drug standard was run along with the tissue section to quality check the MALDI signal.

Creation of Rabbit Model of Intraocular Retinoblastoma

Five New Zealand white rabbits (3 kg) were immunosuppressed with daily subcutaneous cyclosporine injections, as described.[27] Under isoflurane anesthesia, a small sclerotomy was created 2 mm posterior to the limbus in one eye, as previously described. Using a macular contact lens under the operating microscope, 1,000,000 WERI-Rb1 cells were injected under the retina and 1,000,000 WERI-Rb1 cells were injected into the vitreous of the same eye. Retinal tumors and vitreous seed formation were monitored weekly by fundoscopy, fundus photography (either OcuScience, LLC, Henderson, NV, USA; or Apple iPhone (Apple, Cupertino, CA, USA) coupled to a 28D lens; Volk Optical, Mentor, OH, USA), and optical coherence tomography (OcuScience, LLC). Once vitreous seeds and retinal tumors were found to be growing, rabbits were euthanized by barbiturate overdose (125 mg/kg), and both eyes were harvested. The tumor-bearing eye was fixed in formalin, embedded in paraffin, sectioned, and stained with hematoxylin and eosin. Vitreous was sampled from the non–tumor-bearing eye using a 21-gauge needle at the time of euthanasia for determination of vitreous cyclosporine levels by liquid chromatography tandem mass spectrometry, as described above.

Treatment of Intraocular Retinoblastoma by Intra-Arterial Melphalan

Retinoblastoma vitreous seeds were generated by injection of 1,000,000 WERI-Rb1 cells into the vitreous of cyclosporine immunocompromised rabbits, as described above. After 2 weeks of tumor growth, rabbits were treated with either intra-arterial melphalan 3.6 mg or with saline. Rabbits were then euthanized 2 weeks following intra-arterial treatment, and the eyes were removed and fixed in modified Davidson's solution for 48 hours and then transferred to 70% ethanol. Two incisions were made in the globe to create openings to allow processing solutions to flow in and out of the vitreous. Eyes were embedded in paraffin and sectioned at 4 μm. Immunohistochemistry was performed to assess for apoptosis with Caspase-3 antibody (Abcam ab208161; Abcam, Cambridge, MA, USA) at a dilution of 1:100 on the Leica Bond Max Autostainer using H2 antigen retrieval for 20 minutes (Leica Biosystems, Buffalo Grove, IL, USA). This Caspase-3 antibody labels activated Caspase-3 following induction of apoptosis. Slides were evaluated by an experienced veterinary pathologist (KLB).

The melphalan treatment dose was determined as follows. With approval of the Vanderbilt Institutional Review Board and consistent with the tenets of the Declaration of Helsinki, we reviewed the last 50 intra-arterial treatments we performed on our patients, to determine what a clinically relevant dose would be to use in our rabbit experiments. Of these 50 treatments, ~80% involved melphalan. The mean melphalan dose given was 4.1 mg, with an interquartile range of 3.6 to 4.5 mg. We therefore conservatively selected the 25th percentile dose used clinically (3.6 mg) for our in vivo tumor treatment experiments in the rabbits.

Results

Ophthalmic Artery Access and Vascular Supply in Rabbits

The ophthalmic artery could be selectively catheterized for 79 of 79 (100%) eyes in all 47 rabbits. The retinal vasculature was found to arise either predominantly from the EOA off of the ECA (most common variation), or predominantly from the IOA off of the ICA (Fig. 1). Arterial vasospasm was treatable with intra-arterial nitroglycerin.

Assessment of Acute/Subacute Ocular Complications

No vascular occlusions or emboli were noted on fluorescein angiography following selective catheterization (Figs. 2A–2D), and vessels remained patent on posttreatment selective angiography in all cases, without angiographic evidence of vascular occlusion or embolus (Figs. 2E, 2F). For rabbits euthanized 48 hours or 7 days following melphalan treatment, histopathologic assessment of both the treated and untreated eyes showed normal architecture with no evidence of vascular occlusion or retinal damage (Figs. 2G, 2H).

Melphalan Pharmacokinetics

Intra-OA melphalan was delivered successfully to 31 of 31 (100%) eyes. Following unilateral melphalan (0.4 mg/kg) administration, the maximum concentration (C_{max}) observed in the retinal tissue of the treated eye was 4.95 μM, with a time to reach maximum concentration (T_{max}) of 0.5 hours and with an area under the curve from $0 \rightarrow \infty$ ($AUC_{0 \rightarrow \infty}$) of 5.26 μM·h (Fig. 3). For retinal tissue, concentrations in pmol/mg of tissue were converted to μM units, using the assumption that the specific gravity of rabbit retina is ~1 (the specific gravity of normal rat retina has been previously measured at 1.0).[28] The half-life ($t_{1/2}$) of melphalan in the retina of the treated eye was 1.16 hours. In blood plasma, a melphalan C_{max} of 1.04 μM was

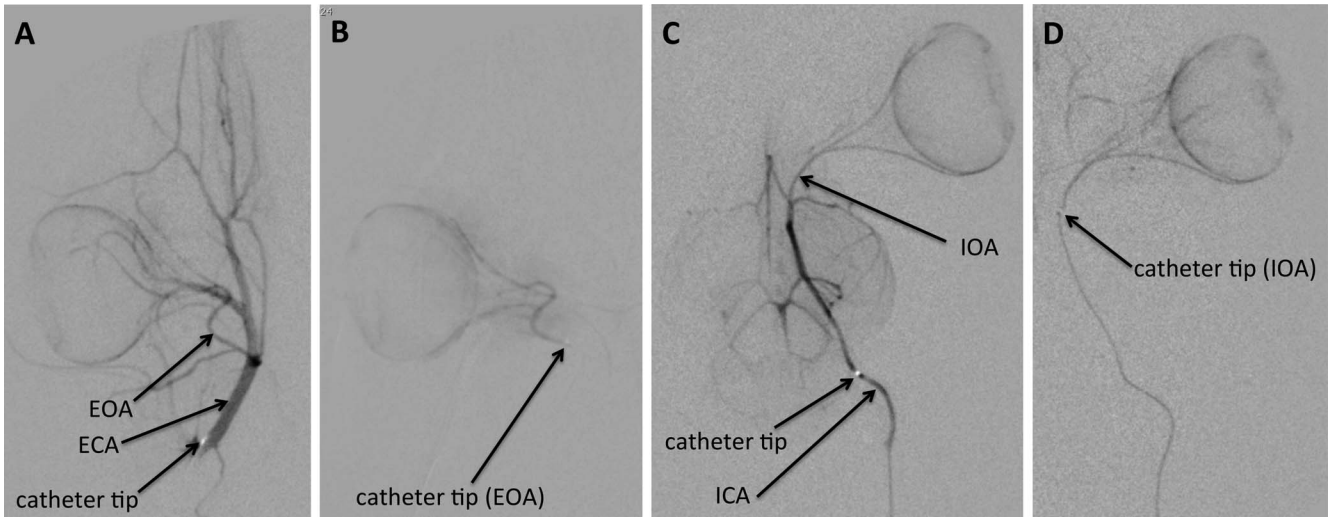

FIGURE 1. Selective arterial angiograms demonstrating selective endovascular ophthalmic artery contrast delivery in rabbits. Retinal and choroidal vasculature arise predominantly from either the external ophthalmic artery arising from the external carotid artery (**A**, **B**) or from the internal ophthalmic artery arising from the internal carotid artery (**C**, **D**). **A** shows the ocular blood supply arising from the external carotid circulation, and **B** demonstrates selective catheterization of the external ophthalmic artery (**A** and **B** both show the same rabbit). **C** shows the ocular blood supply arising from the internal carotid circulation, and **D** demonstrates selective catheterization of the internal ophthalmic artery (**C** and **D** both show the same rabbit). ECA, external carotid artery; EOA, external ophthalmic artery; ICA, internal carotid artery; IOA, internal ophthalmic artery.

reached at a T_{max} of 0.5 hours with an $AUC_{0\rightarrow\infty}$ of 2.07 μM·h, and a half-life of 1.08 hours. In the vitreous of the treated eye, a melphalan C_{max} of 2.24 μM was reached at a T_{max} of 1 hour with an $AUC_{0\rightarrow\infty}$ of 4.19 μM·h and a half-life of 0.83 hours. By contrast, the melphalan concentration in the vitreous of the untreated eye reached a C_{max} of 0.022 μM at a T_{max} of 2 hours and with an $AUC_{0\rightarrow\infty}$ of 0.087 μM·h and a half-life of 2.0 hours (Fig. 3), all consistent with the vitreous of the untreated eye being in equilibrium with blood (see Discussion). Vitreous C_{max} in the treated eye was significantly (100-fold) higher than in the untreated eye ($P = 0.01$), and $AUC_{0\rightarrow\infty}$ in the treated eye was significantly (50-fold) higher than in the untreated eye ($P = 0.01$).

Melphalan Tissue Distribution

Imaging mass spectrometry was performed to determine the relative distribution of melphalan within various ocular structures in a nondisturbed, intact globe. Consistent with our tissue-specific assays, melphalan was found to be present at highest concentration in the retina, compared with the vitreous, with very low levels in avascular structures such as the sclera (Fig. 4).

Rabbit Model of Retinoblastoma With Intraretinal Tumors and Subretinal and Vitreous Seeds

Combined subretinal and intravitreal injections of WERI-Rb1 human RB cells led to the formation of subretinal and intraretinal tumors and vitreous seed clusters, respectively, as has been described previously.[27] Vitreous seeds were observed to grow as clusters within the vitreous, and were clinically visible by 2 weeks after injection (Fig. 5A). Subretinal WERI-Rb1 cell injection led to subretinal tumor formation (Figs. 5B, 5C), as has been reported previously. However, in our hands, this also led to the formation of tumors that were clearly localized to the intraretinal layers, with tumor cells expanding within, and replacing, the normal retinal cellular layers (Fig. 5D). Subretinal and intraretinal tumors were clinically apparent by 2 weeks after injection. Cyclosporine concentrations remained below 2.5 nM in the eyes of all five rabbits.

Efficacy of Intra-Arterial Melphalan Against Retinoblastoma In Vivo in Rabbits

Rabbit eyes bearing retinoblastoma xenografts treated with intra-arterial melphalan displayed widespread induction of apoptosis 2 weeks after treatment as measured by the presence of immunostaining for cleaved caspase-3 (Fig. 6A, 6B). No positive immunostaining was seen in tumor cells in rabbits treated with intra-arterial saline (Fig. 6C). In addition, the vitreous seeds in rabbits treated with saline showed continued growth and expansion compared with the reduction in vitreous seed size and burden seen in those eyes treated with intra-arterial melphalan. This demonstrates that the retinoblastoma tumor cell death is in direct response to the intra-arterial melphalan treatment and not to vascular flow changes associated with the intra-arterial technique itself, nor is this attributable to non–treatment-related apoptosis in the xenografted cells in the rabbit model over time.

DISCUSSION

We describe the first small animal (rabbit) model of IAC. We determined the vitreous and retinal tissue PK in this model and demonstrate excellent vitreous and retinal penetration, regardless of the particular vascular anatomy in each given rabbit. We demonstrate efficacy in killing retinoblastoma xenografts in vivo in rabbit eyes using intra-arterial melphalan, without any acute or subacute ocular complications, thus establishing a model for future drug discovery research.

Currently, advances in the use of IAC have been realized through off-label use of various agents in the clinical setting.[29,30] New drug discovery has been hindered by the absence of a small animal model that allows for intra-arterial delivery of drugs to assess efficacy against RB. There are currently two animal models of IAC, both in large animals in which no RB model exists. Schaiquevich et al. described a porcine model of IAC,[21] and Wilson et al. performed IAC in nonhuman primates.[26] However, the nonhuman primate model developed problems with embolus formation and local complications greater than those seen in humans.[31] In

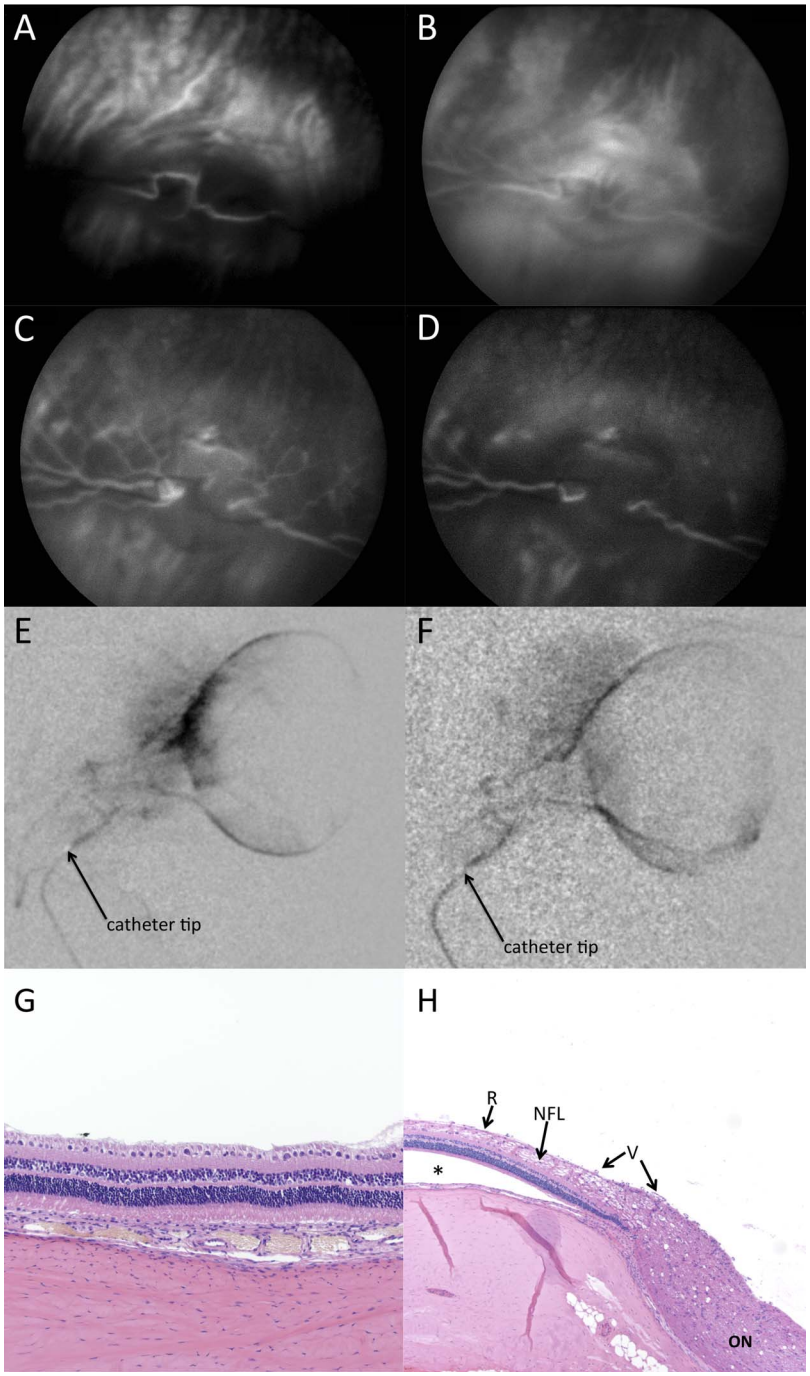

Figure 2. Selective catheterization and intra-arterial chemotherapy delivery did not cause vascular or retinal complications acutely or sub-acutely in our model. (**A–D**) Intra-arterial fluorescein angiograms following selective catheterization of ophthalmic artery, showing choroidal/early arterial phase (**A**), late arterial phase (**B**), transit/early venous phase (**C**), and late venous phase (**D**), demonstrating intact vasculature in each phase without evidence of occlusion. Arterial phase began at 1 second (earliest still image obtained was at 1 second), consistent with direct intra-OA delivery of fluorescein. (**E**, **F**) Intra-arterial delivery of melphalan did not lead to vascular occlusion. Angiograms showing intact vasculature prior to melphalan infusion (**E**) and following melphalan infusion (**F**). (**G**, **H**) Histopathology of treated eyes harvested 48 hours (**G**) or 7 days (**H**) after intra-OA melphalan infusion (1.2 mg). The eyes were fully sectioned, and no sections showed any evidence of ischemia or any sequelae of vascular occlusion. Retinal detachment (indicated by asterisk) is artifactual. R, retina; NFL, nerve fiber layer; V, vessels; ON, optic nerve.

addition, there are currently no RB models in either pigs or in nonhuman primates. Thus, while the PK of intra-arterial drugs can be determined in these models, they are of limited utility in assessing the in vivo efficacy of novel chemotherapeutic agents.

In contrast, a rabbit model of intra-ocular RB does exist.[27] We demonstrate here that the same rabbit model system that can be used for IAC can also be used to generate intra-ocular retinoblastoma tumors. Our approach to xeno-engraftment leads to the establishment of intraretinal tumors, mimicking human disease. In addition, these models generated subretinal tumors, as is seen in patients with exophytic retinoblastoma, as well as vitreous seed clusters, reminiscent of those seen in patients with endophytic retinoblastoma. The relative intraoc-

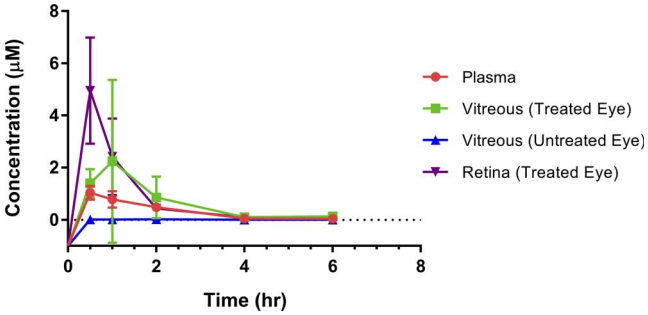

Figure 3. Retinal, vitreous, and plasma pharmacokinetics and tissue drug distribution following selective intra-OA melphalan delivery: 1.2 mg (0.4 mg/kg) of melphalan was infused endovascularly via microcatheter to the OA in a pulsatile fashion over 5 minutes. Animals were euthanized at the specified time points. Vitreous was harvested from both eyes at that time, and the retina was then harvested from the treated eye at that time. A peripheral blood sample was also drawn at the corresponding time point immediately prior to euthanizing the rabbit.

ular tumor burden of retinal tumors and vitreous seeds can be controlled by injecting WERI-Rb1 cells into the subretinal space first, allowing time to grow, and then injecting into the vitreous afterwards (to increase retinal tumor burden), or vice versa (to increase vitreous seed burden), or the initial inoculum of tumor cells can be adjusted. Thus, the ability to deliver chemotherapy drugs into the ophthalmic artery of rabbits in a selective and reproducible fashion will allow for drug discovery in a way not previously possible.

There are several advantages to using rabbits for the assessment of efficacy and toxicity of potential IAC treatments for retinoblastoma: (1) rabbits can be immunosuppressed with cyclosporine to permit xeno-engraftment, as shown here; (2) electroretinography standards are well-known for rabbits, allowing assessment of long-term retinal toxicity[32]; (3) rabbits are an established model organism for many other endovascular neurologic procedures, having been used in dozens of prior studies in the neuro-interventional field[33,34]; and (4) rabbits are readily obtainable for research purposes, and veterinary and husbandry resources are well established, which facilitates larger and more complex studies.

The ultimate goal is to be able to determine the efficacy of various antineoplastic agents against RB for the treatment of retinal tumors and vitreous seeds. Therefore, it is critical to know how long and to what degree tumor cells in the retina or vitreous are exposed to each drug. This will depend on (1) the rate and extent of drug distribution from the blood in the retinal vessels to the vitreous and retina of the treated eye and (2) the rate of elimination from ocular tissues. In the present study, melphalan kinetics were similar in plasma and in the vitreous and retina of the treated eye, with fast distribution (T_{max} ~0.5 to 1 hour) and parallel elimination ($t_{1/2}$ ~0.83 to 1.2 hour). Exposure in the vitreous and retina of the treated eye ($AUC_{0\rightarrow\infty}$ ~4.2 to 5.3 μM·h) was higher than in plasma ($AUC_{0\rightarrow\infty}$ ~2.1 μM·h), as a consequence of the local arterial route of administration. Importantly, vitreous C_{max} of the treated eye was >100-fold higher than the contralateral (untreated) eye's vitreous ($P = 0.01$), and $AUC_{0\rightarrow\infty}$ was ~50-fold higher than the contralateral (untreated) eye's vitreous ($P = 0.01$). In addition, the untreated eye vitreous PK curve remained flat, and the concentration in the untreated eye vitreous remained below the plasma concentration even at the final 6-hour time-point, consistent with equilibrium with systemic blood levels, as is seen with intravenous administration. In contrast, the shape of the PK curve and the high drug concentrations seen in the treated eye reflect local intra-OA

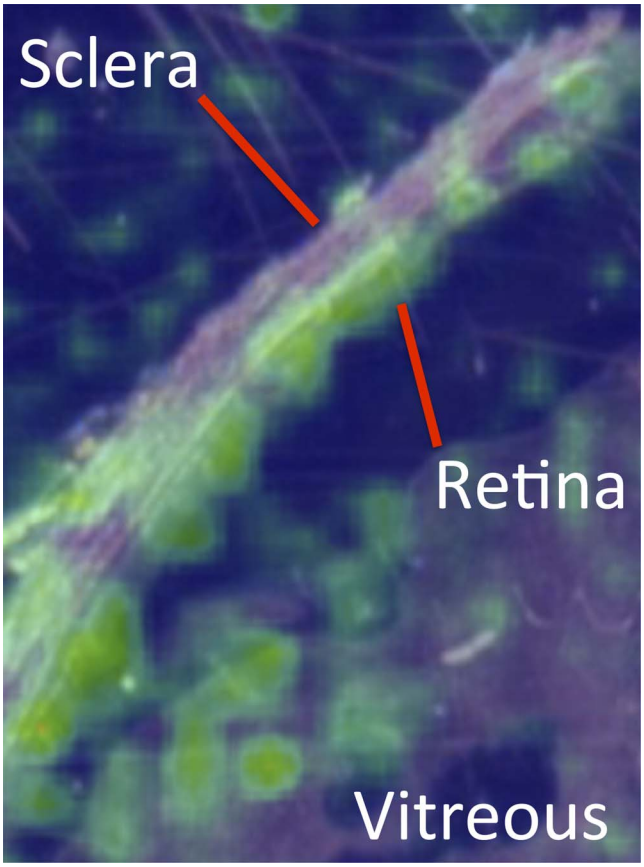

Figure 4. Ocular distribution of melphalan following selective intra-OA infusion. False color map of histology-directed MALDI imaging mass spectrometry data showing relative melphalan levels at different locations in the eye. Note that melphalan localization was greater to the retina than to the vitreous. Minimal drug localized to the avascular sclera.

delivery, rather than systemic recirculation. Specifically, we can assume that systemic recirculation accounts for less than 2% of the drug levels seen in tissues in the treated eye, as the drug levels in the contralateral untreated eye were 2% of those seen in the treated eye. Imaging mass spectrometry likewise confirmed melphalan distribution to retina to a greater extent than to vitreous (Fig. 4).

We injected 1.2 mg melphalan in these 3.0-kg rabbits for the PK experiments, because 0.4 mg/kg is the typical maximal dose used in human patients with retinoblastoma. Of course, most children receiving IAC for retinoblastoma are larger than 3 kg, and so most children would actually receive a higher dose. It is known that eye size and blood flow do not increase as fast as total body size in children. However, it is total body weight that currently limits dosing in humans, as a dose-limiting toxicity of melphalan is myelosuppression. Thus, the eyes of larger children receive a relatively higher dose of chemotherapy, per total body weight.

Along these lines, Schaiquevich et al. injected a much higher dose (7 mg) of melphalan in their 60- to 80-kg porcine model of IAC.[21] Despite the relatively conservative, low dose of melphalan injected in our model, we found that, even at this low dose, the treated eye vitreous and retinal concentrations of melphalan reach levels that are several times higher than the previously published IC_{50} of melphalan for human RB cells.[21] For comparison, in our model, injecting 1.2 mg melphalan into the OA of rabbits leads to a peak vitreous concentration of 2.24 μM, whereas injecting 7 mg melphalan into the OA of Landrace

FIGURE 5. Rabbit xenograft model of retinoblastoma. Growth and formation of retinal tumors and vitreous seeds following combined subretinal/intravitreal injection of WERI-Rb1 human retinoblastoma cells into cyclosporine-immunosuppressed rabbits. (**A**) Fundus photograph clearly demonstrating the formation of vitreous seeds (*arrows*). (**B**) Fundus photograph showing formation of retinal tumor. (**C**) Histology (hematoxylin and eosin) of subretinal tumor (*arrow*) and vitreous seed clusters (*star*). (**D**) Histology (hematoxylin and eosin) demonstrating intraretinal tumor formation, showing expansion and replacement of retinal layers (*arrow*). Retinal detachment is artifactual.

pigs lead to a peak vitreous concentration of only 0.557 μM.[21] This represents a more than fourfold greater peak melphalan concentration, compared with the previously published porcine model. Similarly, in our model, injecting 1.2 mg melphalan into the OA of rabbits leads to a calculated area under the curve of 4.19 μM·h in vitreous, whereas injecting 7 mg of melphalan into the OA of Landrace pigs lead to a calculated area under the curve of only 1.28 μM·h.[21] This represents a more than threefold greater area under the curve, compared with the previously published porcine model, despite giving a much lower injection dose of melphalan in our rabbits. Our peak retinal tissue concentration (4.95 μM) and retinal tissue area under the curve (5.26 μM·h) are even higher still.

We were initially concerned that the small size of rabbits, and the consequent low drug dosages administered (only 1.2 mg at 0.4 mg/kg), might not allow for adequate ocular drug concentrations to be achieved, in contrast to the 7-mg melphalan doses administered to the 60- to 80-kg Landrace pig model. However, as can be seen above, the rabbit actually allows for higher ocular (absolute) drug concentrations than the pig, even when a lower initial dose is administered. It is unclear if this is a species-specific feature, and it is unclear how this compares to human ocular drug penetration. However, as the ultimate goal will be drug discovery, the important feature is that adequate penetration into the rabbit eye is feasible using IAC. We demonstrate that there was no evidence of acute or subacute retinal or vascular damage to the treated eyes using our IAC technique (Figs. 2A–2H). Experiments are underway to determine the maximum nontoxic dose of melphalan that can be given in this rabbit model and to assess for long-term ocular and systemic toxicity of various doses of various drugs in this model system.

Although retinal melphalan levels in the treated eye peaked at the first measured time point (0.5 hours), treated eye vitreous melphalan levels peaked between 0.5 to 1 hour after drug infusion. In our PK experiments, the mid-vitreous was sampled with a needle prior to harvesting the retina. Because drug enters the vitreous via the retinal circulation, it has to transit the vitreous from the retinal surface to the mid-vitreous, which was the location that was sampled. This may explain the consistent finding that vitreous levels of melphalan were moderately lower and peaked slightly later than retinal drug levels. Were total vitreous harvested, we would anticipate that the average concentration would actually be higher than what we report here. However, we felt that a conservative mid-vitreous sample would give a better idea of the minimum melphalan concentration to which vitreous seeds in the mid-vitreous would be exposed.

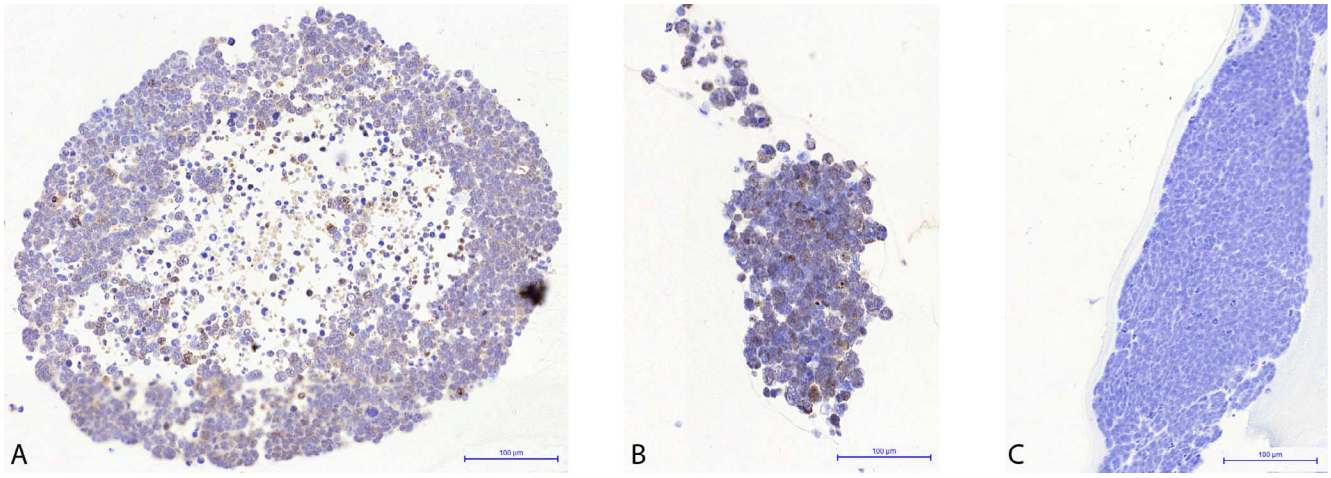

FIGURE 6. Treatment of intraocular RB xenografts with intra-arterial melphalan. Following generation of vitreous seeds, rabbits were treated with either intra-arterial melphalan (**A**, **B**) or intra-arterial saline (**C**) and harvested 2 weeks after treatment. (**A**, **B**) Anti-cleaved Caspase-3 immunostaining of vitreous seeds demonstrating widespread positivity indicative of widespread apoptosis. **A** and **B** show representative seeds from two different rabbits. (**C**) No positive anti-cleaved Caspase-3 immunostaining was seen in eyes treated with intra-arterial saline.

Investigative Ophthalmology & Visual Science

For the first time in an animal model, we demonstrate that intra-arterial melphalan effectively induces widespread apoptosis of intraocular RB xenografts. Importantly, this apoptosis was induced in the vitreous seeds, which we known from clinical practice are notoriously hard to treat. However, the main difference in efficacy between IAC and IV chemotherapy is seen in the ability to treat seeds. Along these lines, we and others have shown that both IAC and IV chemotherapy achieve excellent rates of tumor control for ICRB group A-C eyes (no seeds), whereas IAC achieves much higher levels of globe salvage for group D eyes (with seeds).[15,17,35] In addition, vitreous melphalan levels achieved in our model are lower than those achieved in the retina itself. Thus, we felt that the most compelling efficacy experiments would be to treat seeds in the vitreous with IAC. Widespread apoptosis was induced in eyes treated with intra-arterial melphalan (Figs. 6A, 6B) but not in eyes treated with intra-arterial saline (Fig. 6C). This confirms that the tumor death is due to the drug itself, not due to vascular flow alteration from our technique. Along these lines, larger and more cellular vitreous seeds are seen following saline treatment (Fig. 6C) than are seen in the eyes treated with intra-arterial melphalan, consistent with continued, unimpeded growth in the saline-treated eyes.

In determining the appropriate dose of melphalan to use in the efficacy experiments, we did not want to use an unreasonably high dose of melphalan, as this would not be translatable to the clinic. In reviewing the last 50 IAC treatments we performed on our patients, we determined that 75% of patients who received melphalan received a dose of 3.6 mg or more. We thus selected this dose as the clinically relevant dose, even though our goal in the rabbits was to treat vitreous seeds with a single IAC infusion. Interestingly, most of these patient eyes received this melphalan as part of multi-drug intra-arterial combination therapy, in conjunction with carboplatin and/or topotecan. We also found that of the 18 IAC treatments given to eyes with vitreous seeds present, the doses we used in clinical practice were even higher, with 75% of eyes receiving at least 4 mg of melphalan (usually in combination with carboplatin and/or topotecan). We decided to take a very conservative approach, and thus we selected as our treatment dose in the rabbit experiments the dose of melphalan that represented the 25th percentile of all treated eyes in our practice, namely 3.6 mg, which is lower than what we use to treat those patient eyes that have vitreous seeds present.

There are certain limitations to this rabbit model. The dual internal/external OAs in rabbits differ from the single vessel found in humans. However, we demonstrate here that drug can be effectively infused via either the internal OA or external OA, with excellent vitreous and retinal penetration regardless of vascular anatomy. In addition, rabbit vessels are relatively small and thus selective catheterization can be challenging in inexperienced hands. However, we were able to achieve ophthalmic artery selection in 100% of rabbits. After mastering the technique in the first few animals, we found that we were able to catheterize the rabbit and deliver drug within a matter of minutes. Due to melphalan's relative insolubility, it is known that melphalan begins to come out of solution after an hour.[36] The ease and speed with which intra-arterial microcatheters could be positioned, vascular anatomy explored, and the dominant ophthalmic artery selectively catheterized in our model in our hands allowed multiple rabbits to be treated within this 1-hour window (up to four rabbits within the hour). Another difference is that rabbits are merangiotic, with the retinal vessels lying immediately above the surface of the retina, rather than under the internal limiting membrane as is the case in humans.[37] However, we found that this does not affect consistency of PK or drug penetration for intra-arterially delivered drugs. Rather, we demonstrated excellent vitreous and retinal penetration and PK of melphalan delivered via the intra-arterial route, with minimal drug entering the contralateral eye (Fig. 3). Last, long-term functional studies will need to be performed to identify any late or chronic ocular or systemic side effects of melphalan (or other drugs) in this model system.

Conclusions

We developed the first small animal model of selective intra-OA chemotherapy. This rabbit model gives excellent vitreous and retinal tissue penetration of drug, achieving vitreous and retinal tissue drug levels that have been shown to be sufficient to kill human retinoblastoma cells, without evidence of acute/subacute retinal or retinal vascular complications. In addition, this same rabbit model can be used to create intraretinal retinoblastoma tumors and vitreous and subretinal seeds. We show that these retinoblastoma tumors xenografts can be killed in vivo by administering intra-arterial melphalan, thus demonstrating that the efficacy of drugs can be directly tested in our model system in a way not possible with any previous models.

Acknowledgments

Portions of this work were presented at the Association for Research in Vision and Ophthalmology Annual Meetings in 2016 (Seattle) and 2017 (Baltimore), and at the International Society of Ocular Oncology Meeting in 2017 (Sydney).

Supported by a Career Starter Grant from the Knights Templar Eye Foundation (ABD), the Vanderbilt Faculty Research Scholars program (ABD), a career development award from the Research to Prevent Blindness Foundation (ABD), National Eye Institute Grant 1K08EY027464-01 (ABD), and an unrestricted departmental grant from Research to Prevent Blindness to the Vanderbilt Department of Ophthalmology and Visual Sciences. This work was also supported by a Department of Veterans Affairs Senior Research Career Scientist award (AR) and Vanderbilt Ingram Cancer Center Support Grant CA68485 for core facilities. It was also supported by P41 GM103391-06 and the National Center for Research Resources, Grant UL1RR024975-01, now at the National Center for Advancing Translational Sciences (2 UL1 TR000445-06). The content is the sole responsibility of the authors and does not necessarily represent the official views of the National Institutes of Health.

Disclosure: **A.B. Daniels**, None; **M.T. Froehler**, Medtronic (C, F), Stryker (C, F), Microvention (F), Penumbra (F), Blockade Medical (C), Control Medical (C); **J.M. Pierce**, None; **A.H. Nunnally**, None; **M.W. Calcutt**, None; **T.M. Bridges**, None; **D.C. LaNeve**, None; **P.E. Williams**, None; **K.L. Boyd**, None; **M.L. Reyzer**, None; **C.W. Lindsley**, None; **D.L. Friedman**, None; **A. Richmond**, None

References

1. Murphree AL, Villablanca JG, Deegan WF III, et al. Chemotherapy plus local treatment in the management of intraocular retinoblastoma. *Arch Ophthalmol*. 1996;114:1348–1356.
2. Shields CL, De Potter P, Himelstein BP, Shields JA, Meadows AT, Maris JM. Chemoreduction in the initial management of intraocular retinoblastoma. *Arch Ophthalmol*. 1996;114:1330–1338.
3. Singh G, Daniels AB. Disparities in retinoblastoma presentation, treatment, and outcomes in developed and less-developed countries. *Semin Ophthalmol*. 2016;31:310–316.
4. Kunkele A, Jurklies C, Wieland R, et al. Chemoreduction improves eye retention in patients with retinoblastoma: a report from the German Retinoblastoma Reference Centre. *Br J Ophthalmol*. 2013;97:1277–1283.

5. Chung SE, Sa HS, Koo HH, Yoo KH, Sung KW, Ham DI. Clinical manifestations and treatment of retinoblastoma in Korea. *Br J Ophthalmol*. 2008;92:1180–1184.
6. Berry JL, Jubran R, Kim JW, et al. Long-term outcomes of Group D eyes in bilateral retinoblastoma patients treated with chemoreduction and low-dose IMRT salvage. *Pediatr Blood Cancer*. 2013;60:688–693.
7. Bartuma K, Pal N, Kosek S, Holm S, All-Ericsson C. A 10-year experience of outcome in chemotherapy-treated hereditary retinoblastoma. *Acta Ophthalmol*. 2014;92:404–411.
8. Rodriguez-Galindo C, Wilson MW, Haik BG, et al. Treatment of intraocular retinoblastoma with vincristine and carboplatin. *J Clin Oncol*. 2003;21:2019–2025.
9. Jehanne M, Mercier G, Doz F. Monitoring of ototoxicity in young children receiving carboplatin for retinoblastoma. *Pediatr Blood Cancer*. 2009;53:1162.
10. Jehanne M, Lumbroso-Le Rouic L, Savignoni A, et al. Analysis of ototoxicity in young children receiving carboplatin in the context of conservative management of unilateral or bilateral retinoblastoma. *Pediatr Blood Cancer*. 2009;52:637–643.
11. Shin JY, Kim JH, Yu YS, et al. Eye-preserving therapy in retinoblastoma: prolonged primary chemotherapy alone or combined with local therapy. *Korean J Ophthalmol*. 2010;24:219–224.
12. Gombos DS, Hungerford J, Abramson DH, et al. Secondary acute myelogenous leukemia in patients with retinoblastoma: is chemotherapy a factor? *Ophthalmology*. 2007;114:1378–1383.
13. Zage PE, Reitman AJ, Seshadri R, et al. Outcomes of a two-drug chemotherapy regimen for intraocular retinoblastoma. *Pediatr Blood Cancer*. 2008;50:567–572.
14. Lee V, Hungerford JL, Bunce C, Ahmed F, Kingston JE, Plowman PN. Globe conserving treatment of the only eye in bilateral retinoblastoma. *Br J Ophthalmol*. 2003;87:1374–1380.
15. Turaka K, Shields CL, Meadows AT, Leahey A. Second malignant neoplasms following chemoreduction with carboplatin, etoposide, and vincristine in 245 patients with intraocular retinoblastoma. *Pediatr Blood Cancer*. 2012;59:121–125.
16. Abramson DH, Daniels AB, Marr BP, et al. Intra-arterial chemotherapy (ophthalmic artery chemosurgery) for group D retinoblastoma. *PLoS One*. 2016;11:e0146582.
17. Shields CL, Mashayekhi A, Au AK, et al. The International Classification of Retinoblastoma predicts chemoreduction success. *Ophthalmology*. 2006;113:2276–2280.
18. Shields CL, Honavar SG, Meadows AT, et al. Chemoreduction plus focal therapy for retinoblastoma: factors predictive of need for treatment with external beam radiotherapy or enucleation. *Am J Ophthalmol*. 2002;133:657–664.
19. Abramson DH, Dunkel IJ, Brodie SE, Kim JW, Gobin YP. A phase I/II study of direct intraarterial (ophthalmic artery) chemotherapy with melphalan for intraocular retinoblastoma initial results. *Ophthalmology*. 2008;115:1398–1404.
20. Munier FL, Gaillard MC, Balmer A, et al. Intravitreal chemotherapy for vitreous disease in retinoblastoma revisited: from prohibition to conditional indications. *Br J Ophthalmol*. 2012;96:1078–1083.
21. Schaiquevich P, Buitrago E, Taich P, et al. Pharmacokinetic analysis of melphalan after superselective ophthalmic artery infusion in preclinical models and retinoblastoma patients. *Invest Ophthalmol Vis Sci*. 2012;53:4205–4212.
22. Taich P, Ceciliano A, Buitrago E, et al. Clinical pharmacokinetics of intra-arterial melphalan and topotecan combination in patients with retinoblastoma. *Ophthalmology*. 2014;121:889–897.
23. Schaiquevich P, Ceciliano A, Millan N, et al. Intra-arterial chemotherapy is more effective than sequential periocular and intravenous chemotherapy as salvage treatment for relapsed retinoblastoma. *Pediatr Blood Cancer*. 2013;60:766–770.
24. Marr BP, Brodie SE, Dunkel IJ, Gobin YP, Abramson DH. Three-drug intra-arterial chemotherapy using simultaneous carboplatin, topotecan and melphalan for intraocular retinoblastoma: preliminary results. *Br J Ophthalmol*. 2012;96:1300–1303.
25. Abramson DH, Fabius AW, Issa R, et al. Advanced unilateral retinoblastoma: the impact of ophthalmic artery chemosurgery on enucleation rate and patient survival at MSKCC. *PLoS One*. 2015;10:e0145436.
26. Wilson MW, Jackson JS, Phillips BX, et al. Real-time ophthalmoscopic findings of superselective intraophthalmic artery chemotherapy in a nonhuman primate model. *Arch Ophthalmol*. 2011;129:1458–1465.
27. Kang SJ, Grossniklaus HE. Rabbit model of retinoblastoma. *J Biomed Biotechnol*. 2011;2011:394730.
28. Stefansson E, Wilson CA, Lightman SL, Kuwabara T, Palestine AG, Wagner HG. Quantitative measurements of retinal edema by specific gravity determinations. *Invest Ophthalmol Vis Sci*. 1987;28:1281–1289.
29. Patel M, Paulus YM, Gobin YP, et al. Intra-arterial and oral digoxin therapy for retinoblastoma. *Ophthalmic Genet*. 2011;32:147–150.
30. Francis JH, Gobin YP, Dunkel IJ, et al. Carboplatin +/- topotecan ophthalmic artery chemosurgery for intraocular retinoblastoma. *PLoS One*. 2013;8:e72441.
31. Tse BC, Steinle JJ, Johnson D, Haik BG, Wilson MW. Superselective intraophthalmic artery chemotherapy in a nonhuman primate model: histopathologic findings. *JAMA Ophthalmol*. 2013;131:903–911.
32. Gjorloff K, Andreasson S, Ehinger B. Standardized full-field electroretinography in rabbits. *Doc Ophthalmol*. 2004;109:163–168.
33. Caldwell B, Flores R, Lowery J, Brown AT, Culp WC. Variations in the circle of Willis in the New Zealand white rabbit. *J Vasc Interv Radiol*. 2011;22:1188–1192.
34. Jahan R, Stewart D, Vinters HV, et al. Middle cerebral artery occlusion in the rabbit using selective angiography: application for assessment of thrombolysis. *Stroke*. 2008;39:1613–1615.
35. Shields CL, Jorge R, Say EA, et al. Unilateral retinoblastoma managed with intravenous chemotherapy versus intra-arterial chemotherapy. Outcomes based on the international classification of retinoblastoma. *Asia Pac J Ophthalmol (Phila)*. 2016;5:97–103.
36. Buitrago E, Lagomarsino E, Mato G, Schaiquevich P. Stability of melphalan solution for intravitreal injection for retinoblastoma. *JAMA Ophthalmol*. 2014;132:1372–1373.
37. Tripathi B, Ashton N. Vaso-glial connections in the rabbit retina. *Br J Ophthalmol*. 1971;55:1–11.

Investigative Ophthalmology & Visual Science